

2021-09-10

# Dry and wet deposition of microplastics in a semi-arid region (Shiraz, Iran)

Abbasi, S

<http://hdl.handle.net/10026.1/17540>

---

10.1016/j.scitotenv.2021.147358

Science of The Total Environment

Elsevier BV

---

*All content in PEARL is protected by copyright law. Author manuscripts are made available in accordance with publisher policies. Please cite only the published version using the details provided on the item record or document. In the absence of an open licence (e.g. Creative Commons), permissions for further reuse of content should be sought from the publisher or author.*

1 **Dry and wet deposition of microplastics in a semi-arid region (Shiraz, Iran)**

2

3 Sajjad Abbasi <sup>a,\*</sup>, Andrew Turner <sup>b</sup>

4

5 <sup>a</sup> Department of Earth Sciences, College of Science, Shiraz University, Shiraz 71454, Iran

6 <sup>b</sup> School of Geography, Earth and Environmental Sciences, Plymouth University, PL4 8AA, UK

7

8 \* Corresponding author. Department of Earth Sciences, College of Science, Shiraz University,  
9 71454 Shiraz, Iran.

10 E-mail address: [sajjad.abbasi@shirazu.ac.ir](mailto:sajjad.abbasi@shirazu.ac.ir)

11

12 Accepted in STOTEN 30 April 2021

13 <https://doi.org/10.1016/j.scitotenv.2021.147358>

14

15

16

17

18

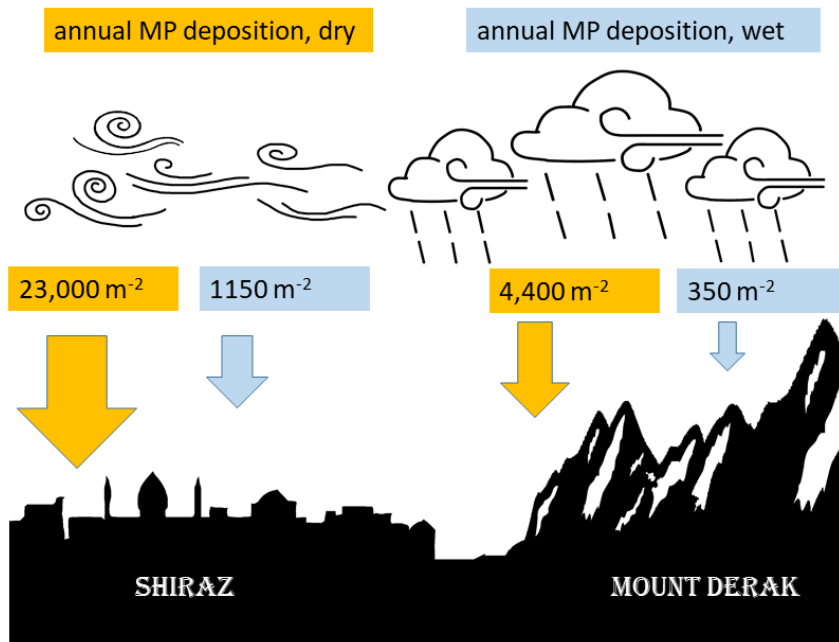
19

20

21

22

23 Graphical Abstract



24

25

26

27

28

29

30

31

32

33

34

35

## 36 **Abstract**

37 Microplastics (MP) have been retrieved from settled dusts and rainfall collected monthly over a period  
38 of a year and daily over an additional period of ten days in the city of Shiraz and at an elevated remote  
39 site (Mount Derak) in Iran. Total monthly deposition of ranged from about 1000 to 3500 MP m<sup>-2</sup> at  
40 Shiraz and about 200 to 600 MP m<sup>-2</sup> at Mount Derak, with greater deposition taking place during the  
41 dry months (June to November) than in months when precipitation events occurred. Overall, MP  
42 deposition was dominated by dry deposition, with precipitation appearing to washout MP and inhibit  
43 local resuspension of material by dampening the ground. The majority of MP in dust and precipitation  
44 (> 99%) were of a fibrous nature, with the finest particles measured (< 100 µm in length) comprising ~  
45 20-40% of MP at Shiraz and ~ 70-80% of MP at Mount Derak and analysis of selected samples (*n* =  
46 34) revealing the most abundant polymers to be polypropylene, polyethylene, and polyethylene  
47 terephthalate. While in Shiraz, local sources of MP are likely significant, the occurrence of MP at Mount  
48 Derak and back trajectories computed with HYSPLIT suggest that distal sources, mainly carried by air  
49 masses from the north and west, are also important. The observations here add to the growing evidence  
50 of the global ubiquity and long-range transport of MP in the atmosphere and reinforce calls for more  
51 research into the potential impacts of MP in this environmental compartment.

52

53 **Keywords:** microplastics; fibres; dust; precipitation; deposition; atmosphere; Iran

54

## 55 **1. Introduction**

56 Microplastics (MP), ranging from 1 µm to 5 mm in size, are generated throughout the life cycle of  
57 plastic products, including production, usage, recycling and disposal. Consequently, they are pervasive  
58 and ubiquitous contaminants of the environment. The concentrations, distributions and impacts of MP  
59 have been well-documented in the marine environment and on marine biota over the past two decades  
60 (Fendall and Sewell, 2009; Cole et al., 2011; Cesa et al., 2017), with scientific attention subsequently

61 extending to freshwater systems (Li et al., 2018; Mendoza and Balcer, 2019) and the terrestrial  
62 environment (Hodson et al., 2017; Machado et al., 2018).

63 Because of their low density compared with soil and dust and, in particular for fibres, their high drag  
64 and low settling velocities, MP are readily emitted to, suspended in and transported by the atmosphere  
65 (Brahney et al., 2020). However, the presence, sources, modelling, impacts and fate of MP in this  
66 environmental compartment have received rather limited and only recent consideration in the literature  
67 (Zhang et al., 2020). Passive samplers have been employed to collect (through wet and dry deposition),  
68 quantify and characterise airborne MP in various urban areas (Dris et al., 2015; Klein and Fischer, 2019;  
69 Stanton et al., 2019; Wright et al., 2020) and at locations remote from any industrial activity or  
70 population centres (Klein and Fischer, 2019; Allen et al., 2020; Brahney et al., 2020) over periods of a  
71 few days to a few months. Detectable MP appear to be dominated by small (sub-mm) fibrous particles  
72 of varying polymeric makeup, with trajectory calculations suggesting both local and distal sources and  
73 the potential for long-range (> 1000 km) transport. A recent study also suggests that MP could be  
74 entering the atmosphere from the ocean (as a secondary source), along with salt and bacteria, through  
75 bubble burst ejection and wave action (Allen et al., 2020).

76 In order to improve our understanding of the transport, deposition and nature of atmospheric MP, we  
77 report on their occurrence in both dry deposition (through gravitational settling) and wet deposition  
78 (with precipitation) from a semi-arid region that experiences distinct climatic seasons. MP are  
79 monitored on a monthly basis over a year and on a daily basis over an additional ten-day period in an  
80 urban location and at an elevated, remote site. MP are classified by size and shape, with a selection  
81 subject to polymeric characterisation, and sources are investigated by computing back trajectories.

82

83

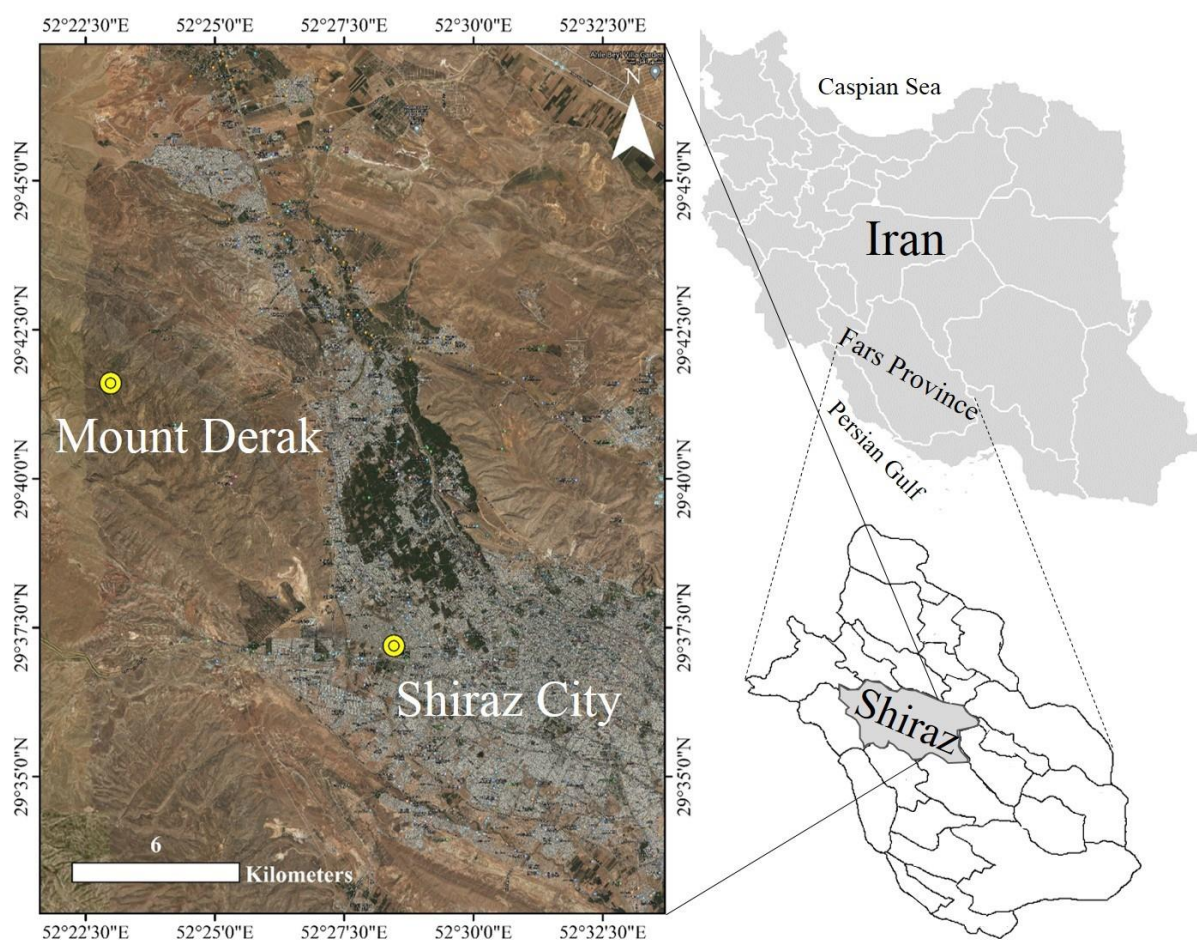
84

85

86 **2. Methods**

87 *2.1. Sample locations*

88 Samples were collected from the urban metropolis of Shiraz, southwest Iran, and a remote but relatively  
89 accessible station on Mount Derak, 20 km to the northwest of the city (Figure 1). Shiraz is the fifth most  
90 populous city in Iran (about 1.9 million in 2016) and lies on a green plain at about 1600 m above sea  
91 level. The city supports an oil refinery and various industries in the electronics, manufacturing and  
92 agriculture sectors. The climate is moderate semi-arid with an annual average rainfall, humidity and  
93 temperature of 335 mm, 64% and 18 °C, respectively, and the prevailing wind direction is from the  
94 northwest. Mount Derak is a sedimentary rock mountain in the Zagros mountain range with a maximum  
95 elevation of 2900 m. The climate here is cooler, wetter and less humid than at Shiraz.



96

97

98

Figure 1: Location of the sampling sites in Shiraz and on Mount Derak.

## 100 2.2. Sampling

101 At both locations, dust and precipitation (mainly rainfall) samples were collected from 1 October 2019  
102 to 30 September 2020 in customised metallic deposition collectors. To obtain enough material and  
103 minimise sample loss during deployment, devices consisted of a wide collection aperture (diameter =  
104 35 cm; area = 0.096 m<sup>2</sup>) connected to a narrow-necked (~ 2 cm diameter) collection bottle. Specifically,  
105 for the collection of dust, the stem of an aluminium foil-wrapped, stainless steel funnel (45°) was  
106 screwed into the neck of a stainless steel bottle, and for the collection of precipitation, the stem of a  
107 shallow (10°), fluted, stainless steel funnel was screwed into the neck of an identical bottle. In Shiraz,  
108 the collectors were secured on to the flat roof of a residential building at about 10 m above ground level,  
109 while on Mount Derak, collectors were fixed on to an outcrop at about 3 m above ground level.

110 By default, collectors for dust were opened and collectors for rain covered with Al foil. On days when  
111 precipitation was forecast (29 occasions throughout the year), dust collectors were manually covered  
112 with Al foil and precipitation collectors were uncovered by an operator wearing cotton clothing. At the  
113 end of each day with precipitation, or within a few hours after rain had ceased, dust collectors were  
114 reopened and precipitation collectors re-covered, after transferring the contents of the latter into a glass  
115 jar via a graduated measuring cylinder. At the end of each month, material accumulated in the dust  
116 collectors (and including the funnel) was transferred into a clean glass jar the aid of a horse-hair brush  
117 and rinsing with filtered water, and between precipitation or dust samples, collector components were  
118 cleaned with multiple rinses of filtered (< 2 µm) water. For a more detailed temporal examination of  
119 dry and wet deposition of MPs, samples were also taken over a period of ten consecutive days (during  
120 March, 2020) consisting of four dry days and six days experiencing precipitation. Monthly or daily  
121 meteorological data were obtained from a gauging station located at Shiraz airport, about 7 km to the  
122 southeast of the city sampling site.

123

## 124 2.3. Sample treatment and microplastic extraction

125 In the laboratory, dust samples were transferred to individual glass beakers using a steel spatula and  
126 dried for 24 h at 25 °C in a cleanroom before being weighed and stored in clean, 60 mL glass beakers  
127 covered with Al foil. Organic matter in the samples was removed by oxidation with 35 mL of 30% H<sub>2</sub>O<sub>2</sub>  
128 (Arman Sina, Tehran) until bubble formation ceased. After allowing dust to settle, residual H<sub>2</sub>O<sub>2</sub> was  
129 decanted and particulate matter washed with deionized water and subsequently dried in a sand bath at  
130 60 °C. MP were isolated by flotation in a saturated solution of ZnCl<sub>2</sub> (Arman Sina, Tehran; density 1.6  
131 – 1.8 g cm<sup>-3</sup>), with the decanted contents centrifuged at 4000 rpm before being filtered through 2 µm  
132 pore size S&S filter papers (blue band, grade 589/3). Filters were air-dried at 25 °C for 48 h in a clean  
133 room and transferred to Petri dishes.

134

#### 135 *2.4. Microplastic counting and characterisation*

136 All MP on each filter were visually identified, counted and characterised under a binocular microscope  
137 (Carl-Zeiss, Köln, Germany) at up to 200-x magnification using a 250 µm-diameter stainless steel probe  
138 and ImageJ software. Identification and characterisation were based on shape, colour, size, thickness,  
139 shininess, hardness and surface structure according to protocols outlined elsewhere and with a size  
140 detection limit of about 20 µm (Abbasi et al., 2019). The polymeric construction of 34 MP of a range  
141 of shapes, sizes and colours and collected over the ten-day sampling campaign was determined using a  
142 micro-Raman spectrometer (µ-Raman-532-Ci, Avantes, Apeldoorn, Netherland) with a laser of 785 nm  
143 and Raman shift of 400-1800 cm<sup>-1</sup>.

144

#### 145 *2.5. Laboratory cleanliness and quality assurance*

146 Laboratory equipment was washed with phosphate-free soap, double-rinsed with filtered water and  
147 soaked in 10% HNO<sub>3</sub> for 24 h before being rinsed twice with double-distilled water, dried at room  
148 temperature in a customised clean room and protected by Al foil. Laboratory work surfaces were  
149 cleaned with ethanol, laboratory clothing was cotton-based and all reagents and solutions were filtered  
150 through 2 µm. Under these conditions, processing of double-distilled water through three blank filters

151 revealed no MP contamination. MP on ten randomly selected dust and precipitation filters were  
152 recounted under the microscope for an evaluation of precision and returned the same values as the  
153 original counts.

154

## 155 *2.6. Trajectory modelling and statistics*

156 The potential source range of MP to the study locations was determined from back trajectory frequency  
157 using the National Oceanic and Atmospheric Administration online software, Hybrid Single Particle  
158 Lagrangian Integrated Trajectory (HYSPLIT), and Global Forecast System (0.25 degree global)  
159 meteorological data. Forty eight-hour air mass backward trajectories were calculated from Shiraz at six-  
160 hour intervals for each month for a height of 500 m above ground level and at a resolution of 1 degree.

161 Statistical tests were performed using the Data Analysis Tool-Pak in Microsoft Excel 2016 with an  $\alpha$   
162 value for significance of 0.05.

163

## 164 **3. Results**

### 165 *3.1. Dry deposition of dust and MP*

166 Table 1 shows the mass of settled dust and the number of MP retrieved from dust during each month of  
167 the year-long sampling campaign and at both sampling locations along with the corresponding  
168 deposition of dust ( $\text{g per m}^2$ ) and the concentration and deposition of MP (per g of dust and per  $\text{m}^2$ ,  
169 respectively). Settled dust deposition in Shiraz averages  $68.3 \text{ g m}^{-2}$  and ranges from  $40.6 \text{ g m}^{-2}$  in March  
170 to  $101.9 \text{ g m}^{-2}$  in September, and the MP concentration averages  $26.4 \text{ MP g}^{-1}$  and ranges from  $17.2 \text{ MP}$   
171  $\text{g}^{-1}$  in May to  $37 \text{ MP g}^{-1}$  in October. Monthly MP deposition averages about  $1900 \text{ MP m}^{-2}$  and ranges  
172 from  $822 \text{ MP m}^{-2}$  in March to  $3494 \text{ MP m}^{-2}$  in September, resulting in a total, annual deposition of about  
173  $23,000 \text{ MP m}^{-2}$ . At Mount Derak, monthly dust deposition averages  $9.1 \text{ g m}^{-2}$  and ranges from  $3.1 \text{ g m}^{-2}$   
174 in March to  $16.6 \text{ g m}^{-2}$  in August, and the MP concentration averages  $43.2 \text{ MP g}^{-1}$  and ranges from  
175  $31.9 \text{ MP g}^{-1}$  in August to  $65 \text{ MP g}^{-1}$  in April. Monthly MP deposition averages  $366 \text{ MP m}^{-2}$  and ranges

176 from 187 MP m<sup>-2</sup> in February to 582 MP m<sup>-2</sup> in October, resulting in a total, annual deposition of about  
 177 4400 MP m<sup>-2</sup>. Also shown in Table 1 is the number of MP collected each month from dust samples at  
 178 Shiraz and Mount Derak that were fibrous in shape. In all cases, fibres of various colours comprised >  
 179 95% of MP, with the remaining particles of a fragmented nature. Overall, > 99% of MP sampled were  
 180 fibrous, whose typical sizes and characteristics are exemplified by the microscopic images in Figure 2.

181

182 Table 1: Monthly quantities and concentrations of settled dust and MP at Shiraz and Mount Derak.

Month	Shiraz						Mount Derak					
	dust, g	dust, g m <sup>-2</sup>	no. MP	no. fibres	MP g <sup>-1</sup>	MP m <sup>-2</sup>	dust, g	dust, g m <sup>-2</sup>	no. MP	no. fibres	MP g <sup>-1</sup>	MP m <sup>-2</sup>
October	8.8	91.5	326	321	37.0	3390	1.2	12.5	56	55	46.7	582
November	7.2	74.9	215	213	29.9	2236	1.1	11.4	42	42	38.2	437
December	5.1	53.0	124	123	24.3	1290	0.9	9.4	35	35	38.9	364
January	4.3	44.7	96	96	22.3	998	0.5	5.2	21	21	42.0	218
February	3.5	36.4	84	83	24.0	874	0.5	5.2	18	18	36.0	187
March	3.9	40.6	79	79	20.3	822	0.3	3.1	19	19	63.3	198
April	5.1	53.0	102	101	20.0	1061	0.4	4.2	26	25	65.0	270
May	6.5	67.6	112	110	17.2	1165	0.6	6.2	25	25	41.7	260
June	7.2	74.9	184	184	25.6	1914	0.8	8.3	34	34	42.5	354
July	8.1	84.2	221	219	27.3	2298	1.2	12.5	42	42	35.0	437
August	9.3	96.7	324	323	34.8	3370	1.6	16.6	51	51	31.9	530
September	9.8	101.9	336	333	34.3	3494	1.4	14.6	53	53	37.9	551
<i>mean</i>	6.6	68.3	184	182	26.4	1909	0.9	9.1	35	35	43.2	366
<i>sd</i>	2.2	22.6	100	99	6.4	1038	0.4	4.4	14	14	10.5	142

183

184

185

186

187

188

189

190

191

192

193

194

195

196

197

198

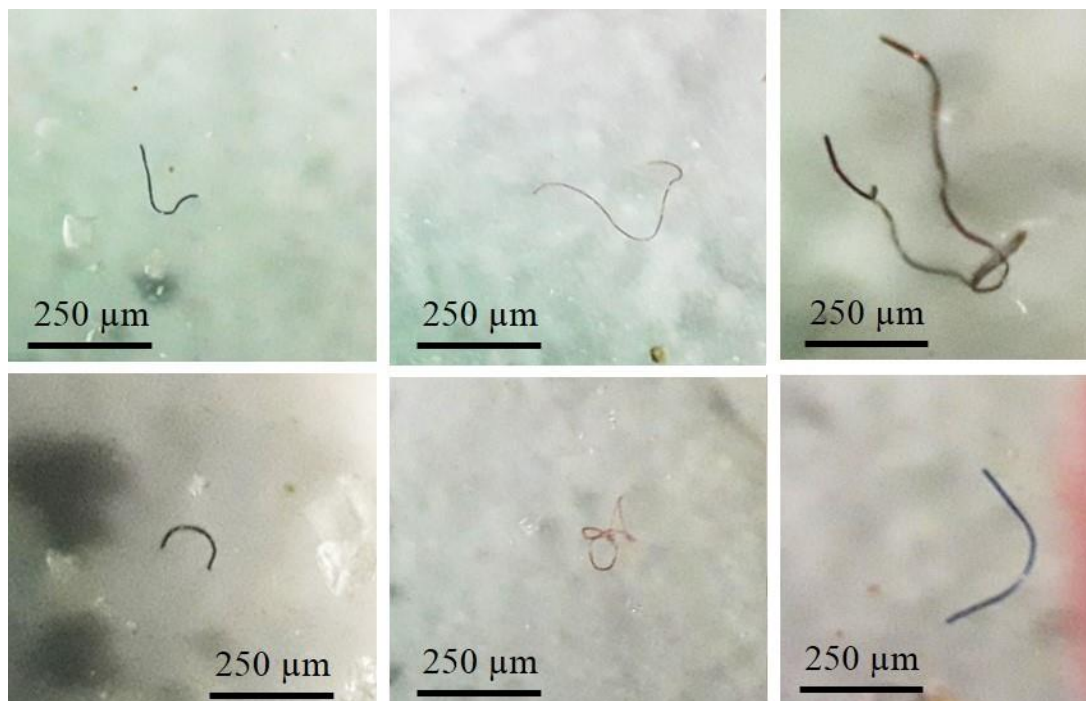


Figure 2: Microscopic images of six fibrous MP retrieved from various settled dust samples.

199

200 *3.2. Wet deposition of MP*

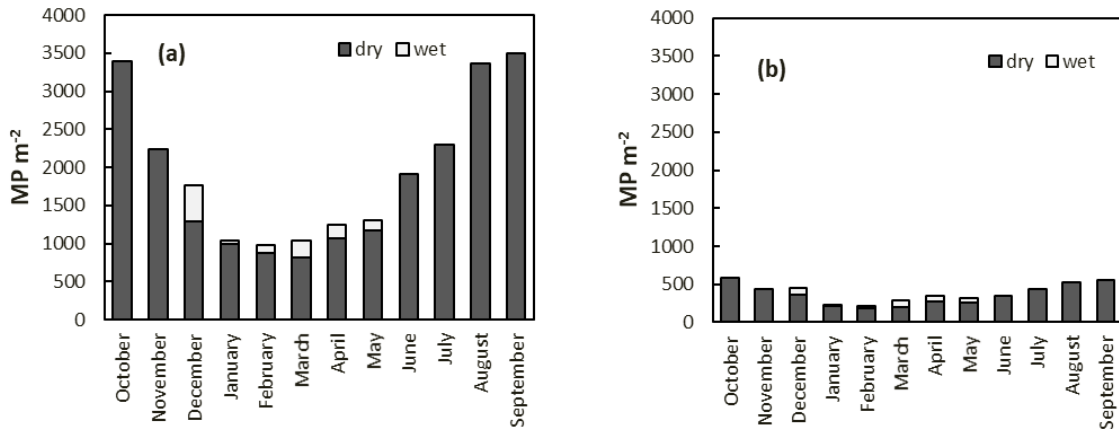
201 Table 2 shows the results for wet MP deposition, along with gauged precipitation data obtained from  
 202 Shiraz airport. Precipitation was recorded and collected in days between December and May, with the  
 203 total number of MP retrieved from Shiraz and Mount Derak ranging from 4 in January to 45 in  
 204 December and from 1 in January to 9 in December and March, respectively. Monthly MP deposition,  
 205 also plotted in Figure 2, ranges from about 40 to 470 MP m<sup>-2</sup> and 10 to 90 MP m<sup>-2</sup> for Shiraz and Mount  
 206 Derak, respectively, while total annual wet deposition is about 1150 MP m<sup>-2</sup> for Shiraz and 350 MP m<sup>-2</sup>  
 207 for Mount Derak. When normalised to volume of precipitation, monthly MP concentrations are < 0.4  
 208 MP mL<sup>-1</sup> for Shiraz with the exception of February (about 2.2 MP mL<sup>-1</sup>) and are < 0.1 MP mL<sup>-1</sup> for  
 209 Mount Derak with the exception of February (about 0.7 MP mL<sup>-1</sup>). Note that, unlike the case for dry  
 210 deposition, all MPs in precipitation samples retrieved from both locations were fibrous.

211 Figure 3 compares the monthly dry and wet deposition of MP at the two locations. Overall, dry  
 212 deposition dominates MP fallout, with wet deposition never contributing more than 30% of total  
 213 monthly deposition. Annually, wet deposition contributes about 5% and 7% towards total MP  
 214 deposition at Shiraz and Mount Derak, respectively.

215

216 Table 2: Monthly precipitation recorded at Shiraz airport and the volumes of precipitation and  
 217 concentrations of MP at Shiraz and Mount Derak.

Month	precipitation, mm	Shiraz				Mount Derak			
		volume, mL	no. MP	MP mL <sup>-1</sup>	MP m <sup>-2</sup>	volume, mL	no. MP	MP mL <sup>-1</sup>	MP m <sup>-2</sup>
October	0	0	0	0	0	0	0	0	0
November	0	0	0	0	0	0	0	0	0
December	73.4	296.4	45	0.15	468	349.5	9	0.03	94
January	12.2	10.5	4	0.38	42	12.3	1	0.08	10
February	5.5	4.5	10	2.22	104	4.4	3	0.68	31
March	57	103.5	21	0.20	218	121.2	9	0.07	94
April	32.7	65.1	17	0.26	177	74.9	7	0.09	73
May	45.5	69.9	14	0.20	146	82.2	5	0.06	52
June	0	0	0	0	0	0	0	0	0
July	0	0	0	0	0	0	0	0	0
August	0	0	0	0	0	0	0	0	0
218 September	0	0	0	0	0	0	0	0	0



219  
 220 Figure 3: Monthly dry and wet deposition of MP in (a) Shiraz and (b) Mount Derak.

221

222 *3.3. Size distribution of MP*

223 Figure 4 shows the monthly size distribution of MP in settled dusts and precipitation. In dust samples,  
 224 the average monthly percentage of the finest fraction of MP (< 100 μm) was significantly greater at  
 225 Mount Derak (74.6) than in Shiraz (31.8) ( $p < 0.01$  according to an independent  $t$ -test). At both  
 226 locations, the percentage of the finest MP was greatest in late winter (February and March) and lowest  
 227 in late summer and early autumn (July through to October). A closer examination of the data revealed  
 228 an inverse relationship between the percentage of fine MP and monthly number of MP (Figure 5). In  
 229 precipitation, the monthly percentage of the finest fraction of MP exhibited no clear temporal trends.  
 230 However, average percentages (92.2 at Mount Derak and 83.7 in Shiraz) were significantly greater than  
 231 the respective average percentages of MP in settle dusts.

232

233

234

235

236

237

238

239

240

241

242

243

244

245

246

247

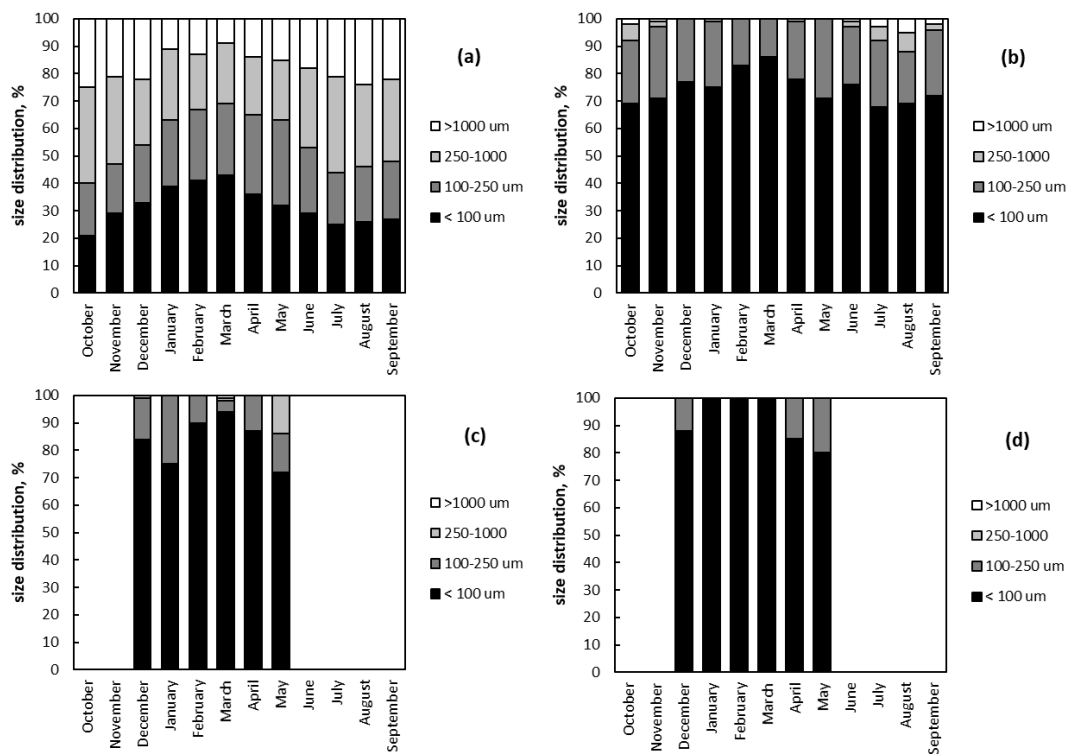
248

249

250

251

252



253 Figure 4: Monthly percentage size distribution of MP in settled dusts from Shiraz (a) and Mount Derak  
254 (b) and in precipitation from Shiraz (c) and Mount Derak (d).

255

256

257

258

259

260

261

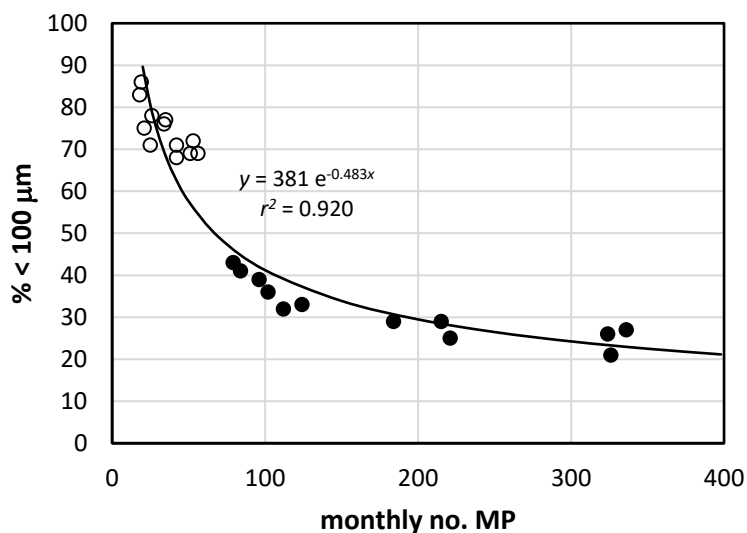
262

263

264

265

266



267 Figure 5: Percentage of MP < 100 μm in length versus monthly number of MP returned for settled dust  
268 samples from Shiraz (●) and Mount Derak (○). Annotated is the best-fit line through the data and the  
269 equation defining the line.

270

271 3.4. Daily MP deposition and polymer type

272 The volumes of precipitation and numbers of associated MP retrieved on ten successive days of  
 273 sampling in March are shown in Table 3. The maximum number of MP deposited in a single day was  
 274 12 (or about 120 MP m<sup>-2</sup>), while on two days in Shiraz and four days at Mount Derak no MP deposition  
 275 was recorded. During spells of continuous precipitation or through successive days in which  
 276 precipitation occurred, and despite variations in the volume of precipitation sampled, there was a  
 277 progressive decline in the daily number of MP recorded.

278

279 Table 3: Daily volume of precipitation and number of MP recovered from Shiraz and Mount Derak.

day	Shiraz		Mount Derak	
	volume, mL	no. MP	volume, mL	no. MP
1	0	2	0	0
2	0	1	0	1
3	7.5	12	8.2	4
4	7.5	2	9.1	1
5	10.5	0	12.0	1
6	62.1	1	75.1	0
7	0	1	0	0
8	0	3	0	1
9	1.8	3	1.8	1
10	1.5	0	2	0

280

281

282 Figure 6 shows the distribution of MP ( $n = 34$ ) collected throughout the ten-day sampling period at  
 283 Shiraz and Mount Derak according to polymer type. Polyolefins and polystyrene are the most abundant  
 284 polymers and account for 85% of all MP considered and all MP analysed from Mount Derak. Remaining  
 285 samples from Shiraz were constructed of polyvinylchloride, polyethylene terephthalate and Nylon.  
 286 Relative polymer abundance also exhibited a significant inverse correlation with material density ( $r = -$   
 287  $0.832$ ;  $p = 0.05$ ).

288

289

290

291  
292  
293  
294  
295  
296  
297  
298  
299  
300  
301  
302  
303  
304  
305  
306  
307  
308  
309  
310  
311  
312  
313  
314  
315  
316  
317

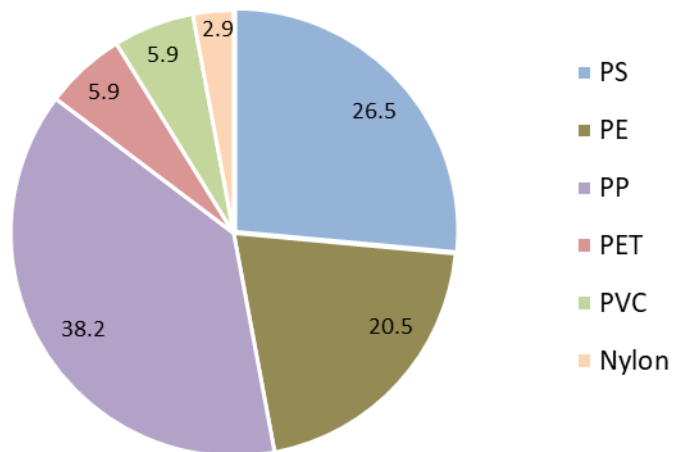
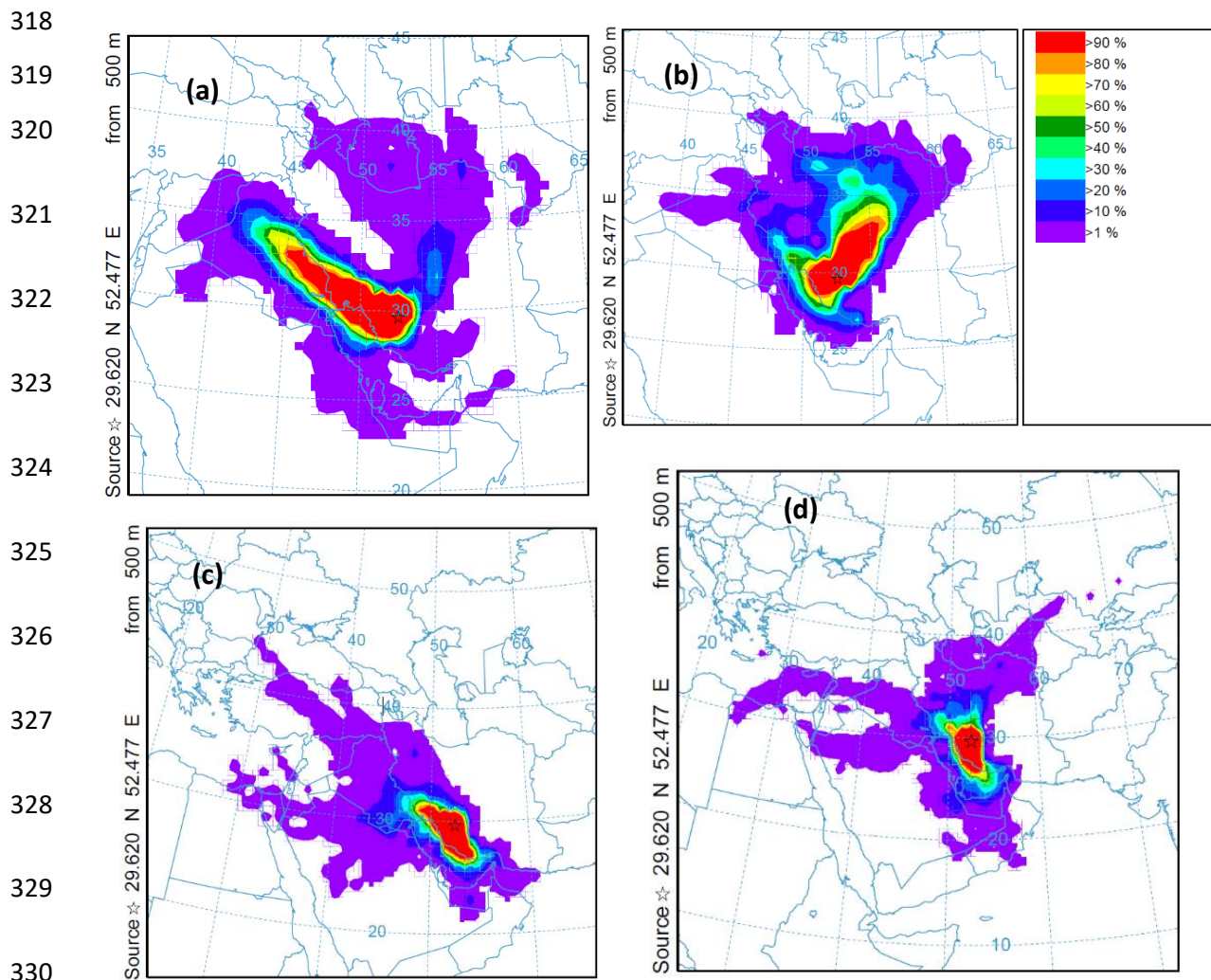


Figure 6: Percentage polymeric distribution of MP ( $n = 34$ ) collected daily from Shiraz and Mount Derak. PS = polystyrene; PE = polyethylene; PP = polypropylene; PET = polyethylene terephthalate; PVC = polyvinyl chloride.

### 3.5. Monthly trajectory frequencies

Examples of monthly trajectory frequencies at Shiraz, calculated using HYSPLIT for 48-h periods and six-h intervals, are shown in Figure 7. In each month illustrated, the geographical range (exceeding 1% frequency) extends to about 2000 km from the city, and mainly in a northerly or westerly direction. During August and September, when MP deposition (per  $m^{-2}$ ) was highest and there was no precipitation, the areas of greatest (> 90%) frequency have a dominantly north-westerly or north-easterly component. In contrast, during February and March, when deposition was lowest and precipitation occurred, the areas of greatest frequency have a more southerly component.



331 Figure 7: Trajectory frequencies calculated for Shiraz using HYSPLIT over a 48-h period and at six-  
332 hourly intervals for (a) August, (b) September, (c) February and (d) March.

333

#### 334 4. Discussion

##### 335 4.1. Spatial variations in dust and MP deposition

336 The quantities and deposition of dust were considerably greater in the city region of Shiraz than in the  
337 remote mountainous region, with differences attributed to the greater abundance and variety of  
338 suspendable material in the urban environment (including soil, construction waste, and vehicle- and  
339 industrially-emitted particulates). Greater deposition of MP and a higher proportion of relatively large  
340 particles in the city setting may be attributed to the proximity of industrial and domestic sources of  
341 plastics, and in particular fibrous plastics of polyolefin or PET construction that are typically used in

342 textiles, furnishings, carpeting and industry (Dris et al., 2017). MP size is also smaller in urban  
343 precipitation than in settled urban dust, presumably because (i) larger MP are not readily scavenged or  
344 encapsulated by rain drops, and (ii) there exists a higher proportion of smaller, lighter MP that evade  
345 gravitational settlement in the higher atmosphere where precipitation is formed or passes. The latter  
346 observation is qualitatively consistent with the more general size-deposition distribution of MP shown  
347 in Figure 5 and with equivalent distributions illustrated in the recent literature by Bergmann et al. (2019)  
348 and Bianco and Passananti (2020). Given such relationships, we predict that where deposition is  
349 relatively low, empirical studies of the kind reported here may significantly underestimate MP (and  
350 nanoplastic) deposition on a number basis.

351 Total MP deposition and average particle size are lower at Mount Derak than in Shiraz, consistent with  
352 the inverse relationships between size and deposition referred to above. Significantly, however, dry MP  
353 deposition normalised to dust mass is greater on Mount Derak than in Shiraz, where the stock of settled  
354 and suspendable dusts is augmented by urban anthropogenic sources. Localised sources of deposited  
355 MP in the more remote location could include fibres from outdoor gear, clothing and recreational  
356 activities (Forster et al., 2020). However, because of the relatively high altitude and prevailing wind  
357 directions (see below), we surmise that the majority of particles deposited on Mount Derak reflect the  
358 longer-range transportation of fine, low density and low settling velocity MP and their subsequent  
359 intersection by the mountain range (see below).

360

#### 361 *4.2. Temporal variations in MP deposition*

362 In the present study, two climatic seasons (cool and wet: December to May; dry and warm: June to  
363 November) were associated with distinctly different patterns of dust and MP deposition at both  
364 locations. Thus, the dry season was accompanied by greater deposition of dust per m<sup>2</sup> and greater  
365 deposition of MP on a number, dust weight-normalised and area-normalised basis. While a significant  
366 fraction of material is likely to have been derived locally in Shiraz, trajectory modelling suggests that,  
367 on Mount Derak, to the north west of the city and remote from any major population centres and

368 industries within 100 km in other directions, significant quantities of MP are sourced from urban areas  
369 farther afield and transported by regional air masses from the north-west and north-east. Brahney et al.  
370 (2020) suggest that the principal source of MP in remote, elevated locations more generally is regional  
371 (up to 1000 km) population centres and urban areas further afield that lie on back trajectories of air  
372 masses.

373 During the wet season, dry deposition of MP was augmented by wet deposition, but the total monthly  
374 deposition of MP remained lower than that in the dry season (Figure 3). Presumably, this is because as  
375 precipitation washes material out from the atmosphere it dampens the ground and inhibits local and  
376 regional resuspension of dust and MP. These effects also account for the progressive reduction in MP  
377 deposition on successive days of precipitation (Table 3). During this season, trajectory modelling  
378 indicates a greater southerly component and a different source of MP in Shiraz and Mount Derak.  
379 Regarding the latter, trajectories suggest a significant fraction of MP may be derived directly from  
380 Shiraz to the south-east. More generally, air masses from this direction have a greater maritime  
381 influence and it is possible that long-range sources could be related to the entrainment of MP from the  
382 ocean into the atmosphere through aerosolisation (Allen et al., 2020).

383 Recent studies in temperate climates have suggested that dry deposition of airborne MP is a significant  
384 contributor to atmospheric fallout (Brahney et al., 2020; Roblin et al., 2020; Szewc et al., 2020). The  
385 current study confirms that this is also the case for a semi-arid region, with precipitation contributing at  
386 most 30% to total monthly deposition and, overall, contributing about 5% and 7% to the annual  
387 deposition of MP at Shiraz and Mount Derak, respectively.

388

#### 389 *4.3. Comparison of dust and MP deposition with previous studies*

390 Monthly quantities of deposited dust in the present study are within the range of values reported for a  
391 variety of locations in central Asia by Groll et al. (2013) ( $< 1$  to  $700 \text{ g m}^{-2}$ ) and in the Arabian peninsula  
392 by Al-Awadhi and Al Shuaibi (2013) and Engelbrecht et al. (2017) ( $4$  to  $320 \text{ g m}^{-2}$ ). Moreover, the  
393 period of maximum dust deposition in Shiraz and Mount Derak (towards the second half of the warm,

394 dry season and when winds have their greatest northerly component) coincides with the highest monthly  
395 accumulations reported for the Arabian coastal zone by Engelbrecht et al. (2017).

396 Regarding the deposition of MP, comparisons with literature data must be undertaken more cautiously  
397 because of differences in sampling periods and designs (for example, wet, dry or combined deposition,  
398 elevation above the ground, sampling construction material) and analytical protocols (and in particular  
399 means of material digestion, density separation, particle size measurement and particle identification).  
400 Thus, some studies report only fibres and neglect other forms of MP (Liu et al., 2020), while other  
401 studies do not clearly or quantitatively discriminate natural and synthetic particles or synthetic and  
402 petroleum-based particles (Dris et al., 2015; Brahney et al., 2020). The latter approach could be  
403 problematic in urban areas where natural or cellulose-based fibres may dominate the pool of deposited  
404 fibrous material (Stanton et al., 2019).

405 With these constraints in mind, total (wet plus dry) monthly numbers of MP deposited in Shiraz and on  
406 Mount Derak are compared with the range of values (or mean values) of MP or microfibrils reported in  
407 the literature in Table 4. Note that where data were reported on a daily or yearly basis, monthly  
408 deposition was derived by multiplication by 30 or division by 12, respectively. For Shiraz, MP  
409 deposition is the same order of magnitude as total monthly values (after any correction for non-  
410 petroleum-based materials) reported for Paris, London, Hamburg and various Chinese cities, but is  
411 greater than that reported for Nottingham (UK) and Gdansk (Poland). Total monthly MP deposition at  
412 Mount Derak is similar to the mean monthly deposition measured in the remote regions of the South  
413 China Sea and the Irish coast, but is lower by more than an order of magnitude than the average monthly  
414 deposition of MP reported for other remote, elevated areas, like the Pyrenees, Harburg Hills and  
415 protected areas of the USA. Part of the discrepancy may be attributed to the inclusion of natural or  
416 synthetic (but non-petroleum-based) fibres amongst the particle cohort and the identification of  
417 additional, primary plastic microbeads whose diameters are dominantly  $< 20 \mu\text{m}$  and that would not be  
418 readily detectable by the methods used in our study (Brahney et al., 2020). Overall, and in both urban  
419 and remote areas where polymeric composition has been determined, there appears to be a

420 heterogeneous assortment of plastics of a range of densities that are suspended in and deposited from  
 421 the atmosphere.

422

423 Table 4: Reports of MP deposition (total, wet or dry) in the literature as minimum, maximum or (in  
 424 parentheses) mean monthly number per m<sup>2</sup>, along with any means of sample digestion and MP  
 425 separation employed and the principal polymers identified. PE = polyethylene; PP = polypropylene; PS  
 426 = polystyrene; PET = polyethylene terephthalate; PVC = polyvinyl chloride; PTFE =  
 427 polytetrafluoroethylene; PA = polyamide; PAN = polyacrylonitrile; EVAC = ethylenevinyl acetate; nd  
 428 = not determined; ns = not stated.

location	deposition	digestion, separation	min, m <sup>-2</sup>	max, m <sup>-2</sup>	% plastic	main polymers	reference
<i>urban</i>							
Paris, France	total	no	870	8400	29	nd	Dris et al. (2015)
Dongguan, China	total	no	5250	9390	23	PE, PP, PS	Cai et al. (2017)
Hamburg, Germany	total	NaClO, Nile Red stain	4080	7830	77	PE, EVAC, PET	Klein and Fischer (2019)
Nottingham, UK	total	H <sub>2</sub> O <sub>2</sub>	1260	2040	2.3	ns	Stanton et al. (2019)
Six coastal cities, China	total	H <sub>2</sub> O <sub>2</sub>	2240	7350	100	nd	Liu et al. (2020)
London, UK	total	methanol, Nile Red stain	17,300	30,200	17	PAN, PET, PA	Wright et al. (2020)
Gulf of Gdansk, Poland	total, wet and dry	no	<30	900	100	PET, PP, PE, PVC	Szewc et al. (2020)
Shiraz, Iran	wet and dry	H <sub>2</sub> O <sub>2</sub> , ZnCl <sub>2</sub>	978	3490	100	PP, PS, PE	This study
<i>remote</i>							
Harburg Hills, Germany	total	NaClO, Nile Red stain	9940	15,360	77	PE, EVAC, PET	Klein and Fischer (2019)
Protected areas of continental USA	wet and dry	no	1440	13,100	ns	PET, Nylon, PP, PE, PTFE	Brahney et al. (2020)
French Pyrenees	total	H <sub>2</sub> O <sub>2</sub> , ZnCl <sub>2</sub>	(11,000)		100	PS, PE	Allen et al. (2020)
South China Sea	total	H <sub>2</sub> O <sub>2</sub>	(~600)		100	nd	Liu et al. (2020)
Irish Atlantic coast	total and wet	Rose Bengal stain	363	465	100	PET, PAN, PE, PP	Roblin et al. (2020)
Mount Derak, Iran	wet and dry	H <sub>2</sub> O <sub>2</sub> , ZnCl <sub>2</sub>	218	582	100	PP, PS, PE	This study

430

#### 431 4.4. Environmental and health impacts of airborne MP

432 The impacts of airborne MP on human health are unclear. Once inhaled, those of the size range  
 433 identified in the present study are likely to be deposited in the upper airways and swallowed into the gut,  
 434 with those of smaller dimensions but evading detection potentially respirable (Wright et al., 2020).  
 435 Airborne MP exposure, however, is likely to be far more significant indoors because of the multitude  
 436 of fibrous and non-fibrous sources of plastic, lack of drivers for dispersion and degradation, and the  
 437 length of time spent inside (Dris et al., 2017; Gaston et al., 2020; Liu et al., 2020).

438 The wide dispersion and lengthy residence times of MP and nanoplastics in the atmosphere not only  
 439 result in global environmental and food-chain contamination (Bergman et al., 2019; Brahney et al.,  
 440 2020; Roblin et al., 2020) but also have the potential to impact on processes taking place in the  
 441 atmosphere. For instance, airborne MP and nanoplastics, despite not being hygroscopic, could act as  
 442 cloud condensing nuclei (Allen et al., 2020). In laboratory studies, Ganguly and Ariya (2019) found

443 that the ice nucleation efficiency of synthesized polyethylene particles was dependent on various  
444 physico-chemical factors, like pH and temperature, and was enhanced in the presence of certain  
445 contaminants or natural (e.g. clay) particulates. It is also possible that nucleation efficiency is enhanced  
446 by microbiological and photochemical alteration of the plastic surface or through the acquisition of  
447 static charge via the triboelectric effect. Since the propensity for airborne MP to act as nucleating agents  
448 has implications for climate change, further research in this area is required.

449

## 450 **5. Conclusions**

451 MP have been detected and quantified in dry and wet deposition in an urban centre (Shiraz) and a  
452 remote, elevated location (Mount Derak) in Iran. Samples were dominated by fibrous particles of  
453 polypropylene, polyethylene and PET construction, and monthly deposition exhibited seasonality on  
454 both a number and size basis, with more MP and of greater average length deposited during the drier  
455 and warmer months. The range of total monthly depositional values (about 1000 to 3500 MP m<sup>-2</sup> and  
456 200 to 600 MP m<sup>-2</sup> in Shiraz and at Mount Derak, respectively) and geographical extents of computed  
457 back trajectories are comparable with data and model outputs reported in the recent international  
458 literature and reinforces the importance of the atmosphere as a vehicle for the global transport of MP.  
459 The health and environmental impacts of atmospheric MP remain unclear but warrant further  
460 investigation.

461

## 462 **Acknowledgements**

463 The authors acknowledge Shiraz University for financial support of the study, and Mr Reza Negarandeh  
464 for assistance with sampling at Mount Derak.

465

## 466 **References**

- 467 1. Abbasi, S., Keshavarzi, B., Moore, F., Turner, A., Kelly, F.J., Dominguez, A.O., Jaafarzadeh,  
468 N., 2019. Distribution and potential health impacts of microplastics and microrubbers in air and  
469 street dusts from Asaluyeh County, Iran. *Environmental Pollution* 244, 153–164.
- 470 2. Al-Awadhi, J. M. and Al Shuaibi, A. A.: Dust fallout in Kuwait city: Deposition and  
471 characterization, *Science of the Total Environment* 461, 139–148.
- 472 3. Allen, S., Allen, D., Phoenix, V.R., Le Roux, G., Jimenez, P.D., Simonneau, A., Binet, S.,  
473 Galop, D., 2019. Atmospheric transport and deposition of microplastics in a remote mountain  
474 catchment. *Nature Geoscience* 12, 339-344.
- 475 4. Allen, S., Allen, D., Moss, K., Le Roux, G., Phoenix, V.R., Sonke, J.E., 2020. Examination of  
476 the ocean as a source for atmospheric microplastics. *PLoS ONE* 15, e0232746.
- 477 5. Bergmann, M., Mützel, S., Primpel, S., Tekman, M.B., Trachsel, J., Gerdts, G., 2019. White  
478 and wonderful? Microplastics prevail in snow from the Alps to the Arctic. *Science Advances*  
479 5, eaax1157.
- 480 6. Bianco, A., Passananti, M., 2020. Atmospheric micro and nanoplastics: An enormous  
481 microscopic problem. *Sustainability* 12, 7327.
- 482 7. Brahney, J., Hallerud, M., Heim, E., Hahnenberger, M., Sukumaran, S., 2020. Plastic rain in  
483 protected areas of the United States. *Science* 368, 1257-1260.
- 484 8. Cai, L., Wang, J., Peng, J., Tan, Z., Zhan, Z. Tan, X., Chen, Q., 2017. Characteristic of  
485 microplastics in the atmospheric fallout from Dongguan city, China: preliminary research and  
486 first evidence. *Environmental Science and Pollution Research* DOI 10.1007/s11356-017-0116-  
487 x.
- 488 9. Cesa, F.S., Turra, A., Baruque-Ramos, J., 2017. Synthetic fibers as microplastics in the marine  
489 environment: A review from textile perspective with a focus on domestic washings. *Science of*  
490 *the Total Environment* 598, 1116-1129.
- 491 10. Cole, M., Lindeque, P., Halsband, C., Galloway, T.S., 2011. Microplastics as contaminants in  
492 the marine environment. *Marine Pollution Bulletin* 62, 2588-2597.

- 493 11. Dris, R., Gasperi, J., Rocher, V., Saad, M., Renault, N., Tassin, B., 2015a. Microplastic  
494 contamination in an urban area: a case study in Greater Paris. *Environmental Chemistry* 12,  
495 592-599.
- 496 12. Dris, R., Gasperi, J., Mirande, C., Mandin, C., Guerrouache, M., Langlois, V., Tassin, B., 2017.  
497 A first overview of textile fibers, including microplastics, in indoor and outdoor environments.  
498 *Environmental Pollution* 221, 453-458.
- 499 13. Engelbrecht, J.P., Stenchikov, G., Prakash, P.J., Lersch, T., Anisimov, A., Shevchenko, I.,  
500 2017. Physical and chemical properties of deposited airborne particulates over the Arabian Red  
501 Sea coastal plain. *Atmospheric Chemistry and Physics* 17, 11467-11490.
- 502 14. Fendall, L.S., Sewell, M.A., 2009. Contributing to marine pollution by washing your face.  
503 *Marine Pollution Bulletin* 58, 1225-1228.
- 504 15. Forster, N.A., Tighe, M.K., Wilson, S.C., 2020. Microplastics in soils of wilderness areas: What  
505 is the significance of outdoor clothing and footwear? *Geoderma* 378, 114612.
- 506 16. Ganguly, M., Ariya, P.A., 2019. Ice nucleation of model nanoplastics and microplastics: A novel  
507 synthetic protocol and the influence of particle capping at diverse atmospheric environments.  
508 *ACS Earth Space Chemistry* 3, 1729-1739.
- 509 17. Gaston, E., Woo, M., Steele, C., Sukumaran, S., Anderson, S., 2020. Microplastics differ  
510 between indoor and outdoor air masses: Insights from multiple microscopy methodologies.  
511 *Applied Spectroscopy* 74, 1079-1098.
- 512 18. Groll, M., Opp, Chr., Aslanov, I., 2013. Spatial and temporal distribution of the dust deposition  
513 in Central Asia—results from a long term monitoring program. *Aeolian Research* 9, 49-62.
- 514 19. Hodson, M.E., Duffus-Hodson, C.A., Clark, A., Prendergast-Miller, M.T., Thorpe, K.L., 2017.  
515 Plastic bag derived-microplastics as a vector for metal exposure in terrestrial invertebrates.  
516 *Environmental Science and Technology* 51, 4714-4721.
- 517 20. Klein, M., Fischer, E.K., 2019. Microplastic abundance in atmospheric deposition within the  
518 Metropolitan area of Hamburg, Germany. *Science of the Total Environment* 685, 96-103.

- 519 21. Li, J.Y., Liu, H.H., Chen, J.P., 2018. Microplastics in freshwater systems: A review on  
520 occurrence, environmental effects, and methods for microplastics detection. *Water Research*  
521 137, 362-374.
- 522 22. Liu, K., Wang, X., Song, Z., Wei, N., Haoda, Y., Cong, X., Zhao, L., Li, Y., Qu, L., Zhu, L.,  
523 Zhang, F., Zong, C., Jiang, C., Li, D., 2020. Global inventory of atmospheric fibrous  
524 microplastics input into the ocean: An implication from the indoor origin. *Journal of Hazardous*  
525 *Materials* 400, 123223.
- 526 23. Machado, A.A.D., Kloas, W., Zarfl, C., Hempel, S., Rillig, M.C., 2018. Microplastics as an  
527 emerging threat to terrestrial ecosystems. *Global Change Biology* 24, 1405-1416.
- 528 24. Mendoza, L.M.R., Balcer, M., 2019. Microplastics in freshwater environments: A review of  
529 quantification assessment. *TRAC – Trends in Analytical Chemistry* 113, 402-408.
- 530 25. Roblin, B., Ryan, M., Vreugdenhil, A., Aherne, J., 2020. Ambient atmospheric deposition of  
531 anthropogenic microfibers and microplastics on the western periphery of Europe (Ireland).  
532 *Environmental Science and Technology* 54, 11100-11108.
- 533 26. Stanton, T., Johnson, M., Nathanail, P., MacNaughton, W., Gomes, R.L., 2019. Freshwater and  
534 airborne textile fibre populations are dominated by ‘natural’, not microplastic, fibres. *Science*  
535 *of the Total Environment* 666, 377-389.
- 536 27. Szewc, K., Graca, B., Dolega, A., 2020. Atmospheric deposition of microplastics in the coastal  
537 zone: Characteristics and relationship with meteorological factors. *Science of the Total*  
538 *Environment* (in press).
- 539 28. Wright, S.L., Ulke, J., Font, A., Chan, K.L.A., Kelly, F.J., 2020. Atmospheric microplastic  
540 deposition in an urban environment and an evaluation of transport. *Environment International*  
541 136, 105411.
- 542 29. Zhang, Y., Kang, S., Allen, S., Allen, D., Gao, T., Sillanpää, M., 2020. Atmospheric  
543 microplastics: A review on current status and perspectives. *Earth-Science Reviews* 203,  
544 103118.